

RIME ICE SHAPE PREDICTIONS USING OPENFOAM

Seghaer EDEEB¹
Atilim University
Ankara, Turkey

Hasan U. AKAY²
Atilim University
Ankara, Turkey

Serkan OZGEN³
Middle East Technical University
Ankara, Turkey

ABSTRACT

Aircraft ice accretion starts when an aircraft flies through clouds containing supercooled liquid water droplets. Supercooled droplets have a temperature below the freezing point but are in the liquid phase. Ice grows when the water droplets impinge and freeze on the frontal regions of unprotected aircraft surfaces. The accumulated ice on the aircraft surfaces reduces the maximum lift force, raises the drag force and degrades the aircraft performance. A CFD simulation package created using the suitable modules of the OpenFOAM software is used in this study to predict the rime ice shapes of the ice accretion process and to evaluate its effect on aerodynamic performance. Results show a good agreement of OpenFOAM ice shape predictions for two rime ice cases with the corresponding data in the literature as well as the results of a commercial package ANSYS-FENSAP.

INTRODUCTION

Ice accretion on aircraft surfaces occurs when there are clouds containing supercooled water droplets and ambient temperature is below the freezing temperature. Droplets stay in the liquid phase at a temperature range of -40 °C to 0 °C because of the absence of solid objects. Solid objects such as salt crystals, dust and smoke particles are the nuclei required for the solidification phenomena. Ice accretion and solidification process on the aircraft surfaces takes place as soon as the water droplets hit the solid surfaces. Due to ice accretion, the aircraft aerodynamic shape changes and the aircraft weight increases. This leads to reduction in lift force and an increase in drag force, which have serious effects on the aircraft performance [Beld, 2013].

Numerical computations of aircraft ice accretion have become an important tool in ice shape prediction, design, and certification of flight in icing conditions. Ice accretion simulation can be achieved with a process with many stages. These stages consist of fluid flow simulations, droplet trajectory calculations, thermodynamic predictions, ice accretion calculations, the geometry updating [Heinrich, 1991]; and repeating the same cycle of computations by starting with flow simulations until the required convergence is reached.

¹Ph.D Student, Modeling and Design of Engineering Systems, Atilim University, Email: edeeb.seghaer@student.atilim.edu.tr

²Professor of Mechanical Engineering, Atilim University, Email: hasan.akay@atilim.edu.tr

³Professor of Aerospace Engineering, Middle East Technical University, Email: serkan.ozgen@ae.metu.edu.tr

In this paper, the appropriate modules of OpenFOAM have been modified and integrated to perform full prediction of ice accretion. Since this development is still continuing, only rime-ice predictions have been considered here. The prediction of the more difficult case of glaze ice phenomenon will be addressed later. For the test cases chosen, the obtained results show a good agreement of OpenFOAM ice shape predictions for two rime ice cases with the corresponding data in the literature [Wright et al., 1997] as well as the results of a commercial package ANSYS-FENSAP [ANSYS, 2017].

Main Icing Factors

The main factors affecting the icing process are liquid water content (LWC), ambient temperature and water droplet diameter (MVD). The liquid water content is the measure of the mass of the liquid water in a cloud in a specified volume of dry air. Ambient temperature affects both the severity and the type of ice formed on the aircraft when it is exposed to liquid water droplets. Water droplets are found in liquid phase at temperatures from $-20\text{ }^{\circ}\text{C}$ to $0\text{ }^{\circ}\text{C}$ as supercooled water droplets. Mixture of supercooled water droplets and ice crystals are found at temperatures below $-20\text{ }^{\circ}\text{C}$ and ice crystal particles only at temperatures $-40\text{ }^{\circ}\text{C}$ or lower are found. Droplet median volume diameter (MVD) is also an important factor affecting the icing process. The most usual icing is associated with cloud water droplets of size smaller than 50 microns MVD. In some cases the clouds contain supercooled large droplets (SLD) with MVD higher than 50 microns [Alzaili, 2012].

Icing Types

Accreted ice on the aircraft surfaces is divided into two types, rime ice and glaze ice. The main difference between them is the freezing fraction factor, which is the ratio of solidified mass to the total impinging mass of supercooled water droplets. Rime ice typically forms at low ambient temperature, low liquid water content (LWC) and low droplet median volume diameter (MVD). It is formed when supercooled droplets impinge the wing leading edge and freeze immediately and totally. Rime ice is characterized by low density, opaque, soft, milky appearance and exhibits streamlined shapes. Glaze ice is formed at ambient temperatures just below the freezing temperature, high air liquid water content, high relative impact speed and large water droplet diameter. Supercooled droplets in this type do not freeze totally on the impingement zone. Part of water droplets stay in liquid phase and run back along the surface some distance and freeze. The glaze ice is characterized by higher density, transparent and irregular shape with protrusions [Rong, 1991].

OpenFOAM Software

OpenFOAM software is one of the major open-source software packages used for simulating a variety of problems in continuum mechanics [Jasak, 2009]. OpenFOAM includes specialized solvers for incompressible flow, compressible flow, conduction heat transfer, conjugate heat transfer, electrodynamics, solid dynamics, etc. In this study, OpenFOAM solvers are used to predict the aircraft icing problem in an integrated fashion. Several finite element or finite volume based aerodynamic solvers can be used such as potentialFoam for potential flow, simpleFoam for viscous incompressible flow and sonicFoam for viscous compressible flow. For flow simulations of ice accretion here, we use the incompressible flow code simpleFoam, since the ice accretion phenomena occur in incompressible regimes. A Lagrangian solver such as icoUncoupledKinematicParcelFoam solver is used to simulate the droplet trajectories. The solving process in OpenFOAM are controlled and modified by using three input files: fvSchemes file for selecting discretization schemes, fvSolution file for relaxation and conversion parameters and controlDict file for controlling the simulating time and output data [Greenshields, 2015].

METHOD

Numerical simulation methodology of ice accretion process on the unprotected aircraft surfaces consists of the following stages: creation of the computational geometry of the domain and generation of the computational grid, droplet trajectory calculations, thermodynamic analysis, ice thickness calculations, modification of the boundary of the iced geometry, and determination of degradation in the aerodynamic performance. A schematic diagram of the sequence of these stages is given in Figure 1.

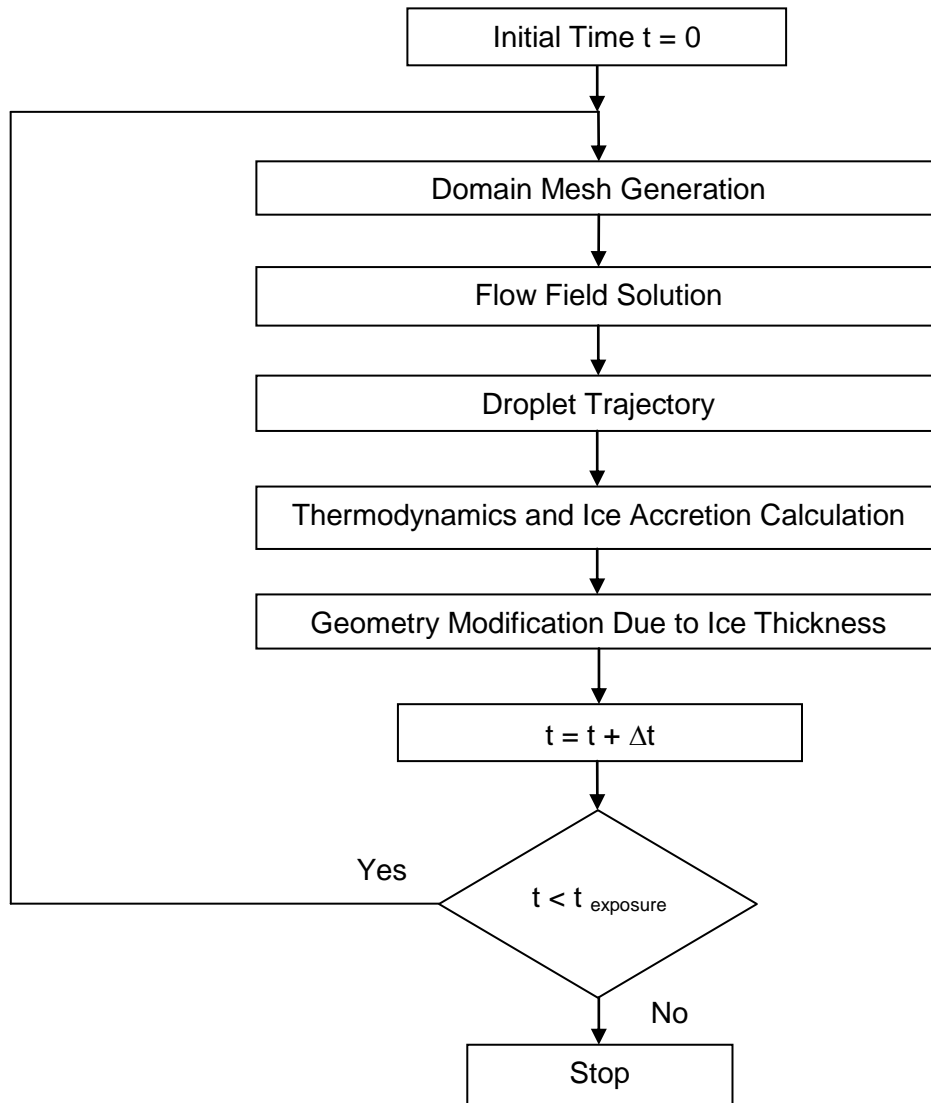


Figure 1: Flowchart of the ice accretion simulation procedure

Test Cases Used for Code Verification

For verification of the procedure developed and integrated in this study, the DRA/NASA/ONERA collaborative icing research test cases are used [Wright et al., 1997]. The boundary conditions for the icing free stream conditions are described by the parameters in Table 1.

Table 1: Ambient and flight conditions used for rime ice shape prediction using OpenFOAM

NASA Cases	Airfoil	Chord (m)	AOA (deg)	Velocity (m/s)	Static Temperature (° C)
27	NACA 0012	0.53	4	58.1	-27.8
33	NACA 0012	0.53	4	93.89	-30.5
NASA Cases	Static Pressure (Pa)	Humidity (%)	LWC (g/m ³)	MVD (microns)	Exposure Time (s)
27	95,610	100	1.3	20	480
33	92,060	100	1.05	20	372

Fluid Flow Simulation Using OpenFOAM Solver

The geometry of the computational domain around airfoil NACA 0012 and the mesh generation is done using open source code GMSH software. A two-dimensional mesh of tetrahedral cells with one layer in the depth direction is generated. A simpleFoam solver is one of the OpenFOAM aerodynamic solvers. It is a steady state, incompressible, laminar and turbulent flow solver. The simulation cases are considered for two dimensional cases so there are no computations done in z-direction. The mesh file created using GMSH with its boundary conditions is converted to foam format. A polyMesh folder is created after the conversion process and the boundary patch types in boundary file must be adjusted. Solution of the incompressible flow around airfoil starts with defining three folders in the incompressible solver in OpenFOAM. Folders named 0, constant, and system must be modified according to the current case. In 0 folder, the initial values for pressure p, velocity U, and turbulent viscosity parameters nut and nuTilda are filled at all boundary conditions for the simulated cases. The boundaries of computational domain are defined by inlet, outlet, topandbottom, frontandback, and airfoilwall surfaces. All physical properties must be defined at these boundaries. The main variable parameters for these cases are defined at the inlet and outlet boundaries by free stream properties as velocity and pressure. Airfoil wall is defined by no-slip condition, and the command empty for the faces in z-direction. Constant folder has polyMesh folder which defines the meshing process completely. Transport and turbulence properties are also defined in the constant folder. The system folder has three control files. These are fvSchemes, fvSolution, and controlDict files. In OpenFOAM, functions can be added to the controlDict file for computing aerodynamic forces and coefficients. Spalart-Allmaras model is used to simulate turbulent flow properties. Gauss linear and gauss linear upwind schemes are used for discretization of the Navier-Stokes equations. SIMPLE (Semi-Implicit Method for Pressure-Linked Equations), GAMG (Generalized geometric-algebraic multi-grid), and Gauss Seidel methods are used for solving the governing equations and for smoothing the solution.

Trajectory Solver

Air velocity distribution in the computation domain obtained from the flow field solution is used for calculating the trajectories of the supercooled water droplets. OpenFOAM solver icoUncoupledKinematicParcelFoam is used to simulate the water droplet trajectories. It is based on Lagrangian approach. The governing equations for this solver are functions of drag, buoyancy and gravity forces. The supercooled water particles in this solver are assumed to be spherical in shape, there is no collision or coalescence between them and

they don't influence the flow field. By solving the governing equations, the solver calculates the droplet trajectory, predicts the impingement zone limits and the collection efficiency parameter can be calculated.

In Lagrangian approach, each droplet trajectory is calculated from Newton's second law of motion based on drag and gravity forces as shown in Figure 2. The governing equations of the droplet trajectories in two-dimensions are given in equations (1) and (2).

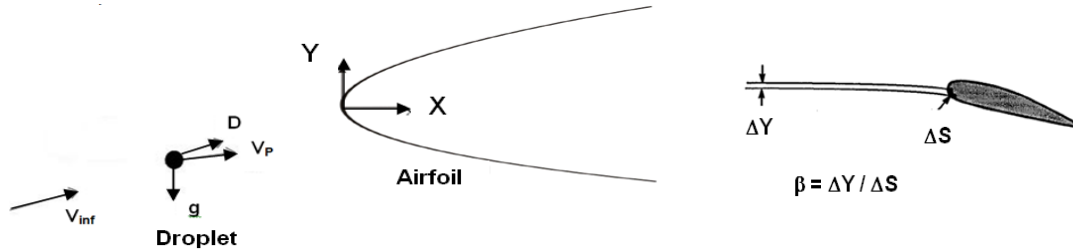


Figure 2: Droplet trajectory

$$m \frac{d^2 x_p}{dt^2} = -D \cos \gamma + mg \sin \alpha \quad (1)$$

$$m \frac{d^2 y_p}{dt^2} = -D \sin \gamma - mg \cos \alpha \quad (2)$$

$$\gamma = \tan^{-1} \left(\frac{(\dot{y}_p - v)}{(\dot{x}_p - u)} \right) \quad (3)$$

where u , v are the components of flow velocity at the droplet position, \dot{x}_p , \dot{y}_p are the components of droplet velocity, γ is the angle between the droplet velocity and air flow velocity; α is the angle of attack.

The drag force (D) is a function of drag coefficient (C_D)

$$D = \frac{1}{2} \rho V^2 A_p C_D \quad (4)$$

The relative velocity is a function of air and droplet velocities:

$$V = \sqrt{(\dot{x}_p - u)^2 + (\dot{y}_p - v)^2} \quad (5)$$

The drag coefficient C_D is based on Reynolds number (Re) [Gent et al., 2000]

$$C_D = \frac{24}{Re} (1 + 0.197 Re^{0.63} + 2.6 * 10^{-4} * Re^{1.38}), \quad Re \leq 3500 \quad (6)$$

$$C_D = \frac{24}{Re} (1.699 * 10^{-5}) Re^{1.92}, \quad Re > 3500 \quad (7)$$

Collection Efficiency (β) is given as [Da Silveira and Maliska, 2001]

$$\beta = \frac{\Delta Y}{\Delta S} \quad (8)$$

where ΔY is free stream water flux per unit area, and ΔS is the surface water flux per unit area.

RESULTS AND DISCUSSION

Fluid Flow Simulation Results

Paraview program is a post processing tool coupled with OpenFOAM software. Paraview program is capable of dealing with complicated geometries and large amount of data. When the simulation solution is converged, residuals criterion of the simulation process is checked, pressure coefficient from pressure distribution around the airfoil is computed, and the aerodynamic coefficients are also checked and compared with literature data for each case. The analysis of different contours and pressure coefficients around the airfoil surface indicate that the obtained results are logical and reasonable.

Figure 3 shows the computational domain grids which are used in the simulation of air flow field and water droplet trajectory. Reynolds number (Re) and Mach number (M) for both cases are: $Re = 3.079 \times 10^6$, $Mach = 0.185$ for Case-27, and $Re = 4.976 \times 10^6$, $Mach = 0.301$ for Case-33. The steady state values of aerodynamic coefficients for both cases 27 and 33 are achieved using OpenFOAM. Lift force coefficient and drag force coefficient values are taken after a number of iterations of 3000. Table 2 shows that the obtained values using OpenFOAM are in good agreement with the corresponding experimental data [Ladson, 1988] in lift coefficients and somewhat overestimated values in drag coefficients. The discrepancy in drag values is resulted due to the use of Spalart-Allmaras turbulent model which gives overestimation in drag coefficient values. The second reason is the limited capability of GMSH program in refining mesh grids close to the airfoil surface. The available experimental data are: $CL = 0.4457$ and $CD = 0.00663$ at $Mach = 0.2$, $Re = 2.66 \times 10^6$ and $AOA = 4.27$ degrees and $CL = 0.4452$ and $CD = 0.00728$ at $Mach = 0.3$, $Re = 4.95 \times 10^6$ and $AOA = 4.03$ degrees.

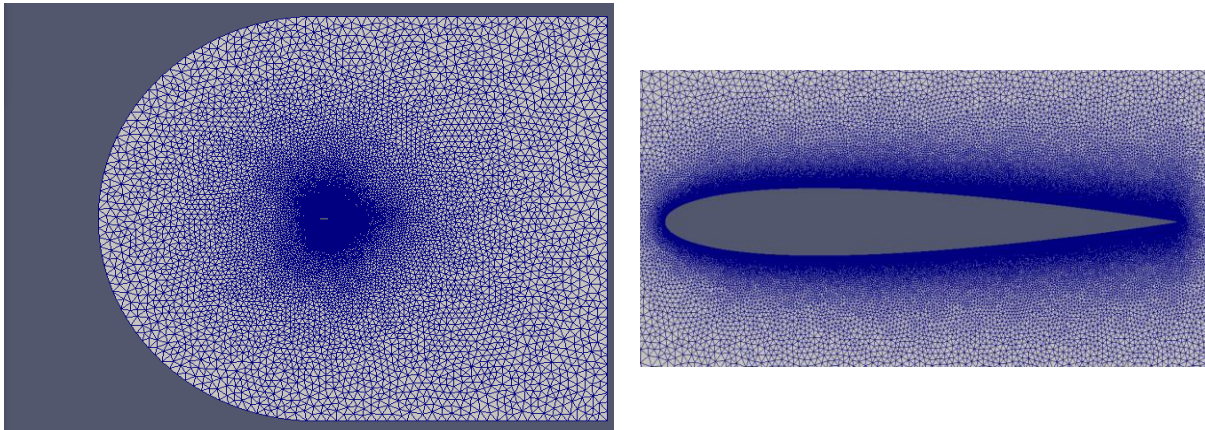


Figure 3: Mesh generation around NACA 0012

Table 2: Comparison of OpenFOAM aerodynamic coefficients with experimental data of clean airfoil NACA 0012 at +4 degrees angle of attack

Case-27		Experimental data	
M = 0.185, AOA = +4 deg		M = 0.2, AOA = +4.27 deg	
CL_OpenFOAM	CD_OpenFOAM	CL_Exp	CD_Exp
0.4341	0.03201	0.4457	0.00663
Case-33		Experimental data	
M = 0.301, AOA = +4 deg		M = 0.3, AOA = +4.03 deg	
CL_OpenFOAM	CD_OpenFOAM	CL_Exp	CD_Exp
0.4320	0.02705	0.4452	0.00728

Trajectory Simulation Results

OpenFOAM Lagrangian solver `icoUncoupledKinematicParcelFoam` is selected. It is a transient solver for the passive transport of a single kinematic particle cloud. It needs flowfield solution as pre-requested data. For multi-time steps, this solver can be used after flow field calculation for each time step. It is one way coupling, where there is no effect of water droplets on the air flow. It has a high capability of coupling with the flow field variables. Many parameters of this solver can be modified such as: particle cloud properties, particle positions, collision between particles [Greenshields, 2015], [Greenshields, 2015], [Da Silveira et al., 2003].

In OpenFOAM, Lagrangian solver `icoUncoupledKinematicParcelFoam` solves the equations of motion of water droplets. Their motion starts when water droplets which are arranged in one line at an upstream position are released and then tracking them until the impacting region. The equations of droplet motion takes gravitational, buoyancy, and drag forces into account. The obtained output data of trajectory calculations are the number of impacting droplet, mass of impacting droplets, and their locations on the airfoil surface. By using Paraview program, the coordinates of the impacting droplets are extracted and used to find an important icing parameter which is the collection efficiency (β). Figures 4 and 5 display the impacting location of water droplets on the airfoil surface for both cases after trajectory solving with one, two, four and six time steps. Figures 6 and 7 show the collection efficiency distributions on airfoil surface of both cases with four time steps. In both figures, collection efficiency plot versus S/C parameter which is the distance measured from the airfoil leading edge along the upper and lower airfoil surfaces per airfoil chord length. As the number of time steps increases, the smoothness of the collection efficiency curves is lost due to ice accretion.

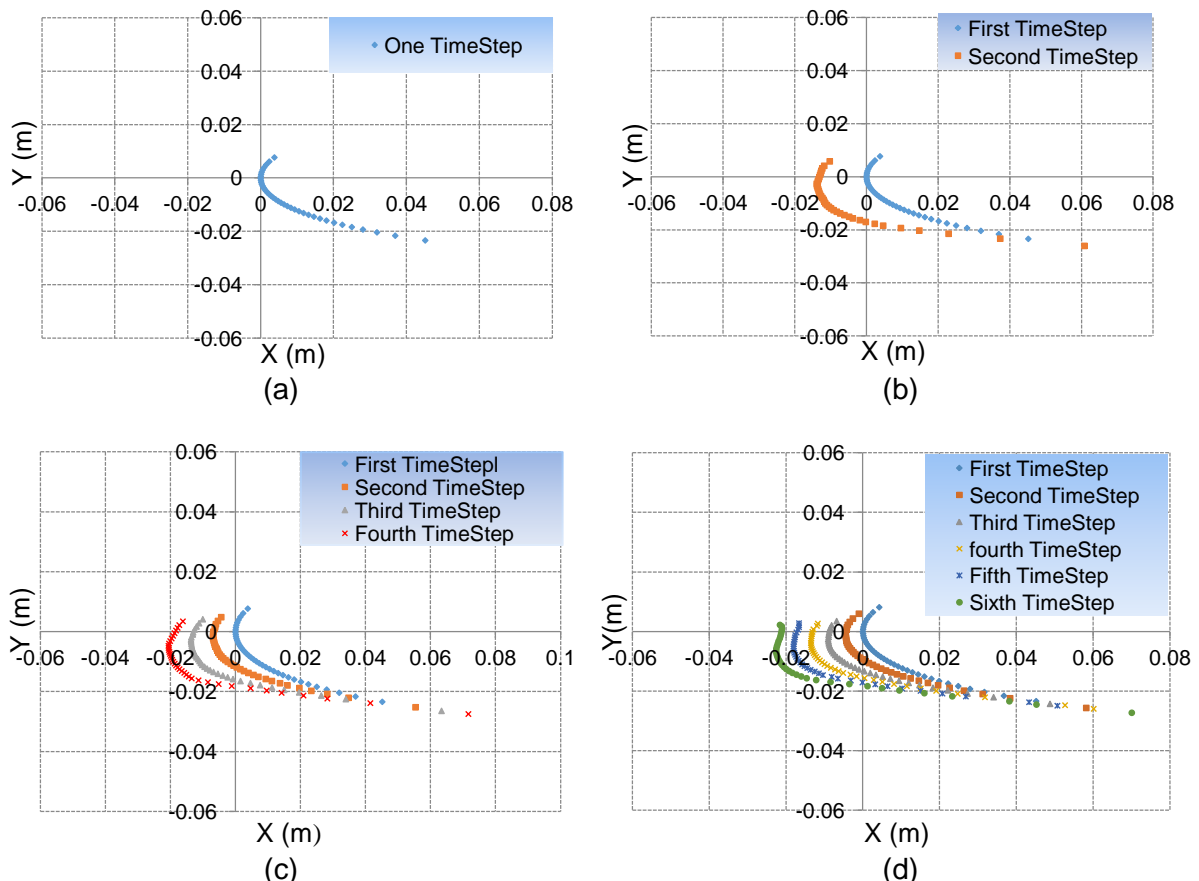


Figure 4: Location of impingement regions for Case-27 with
a) one, b) two, c) four and d) six time steps

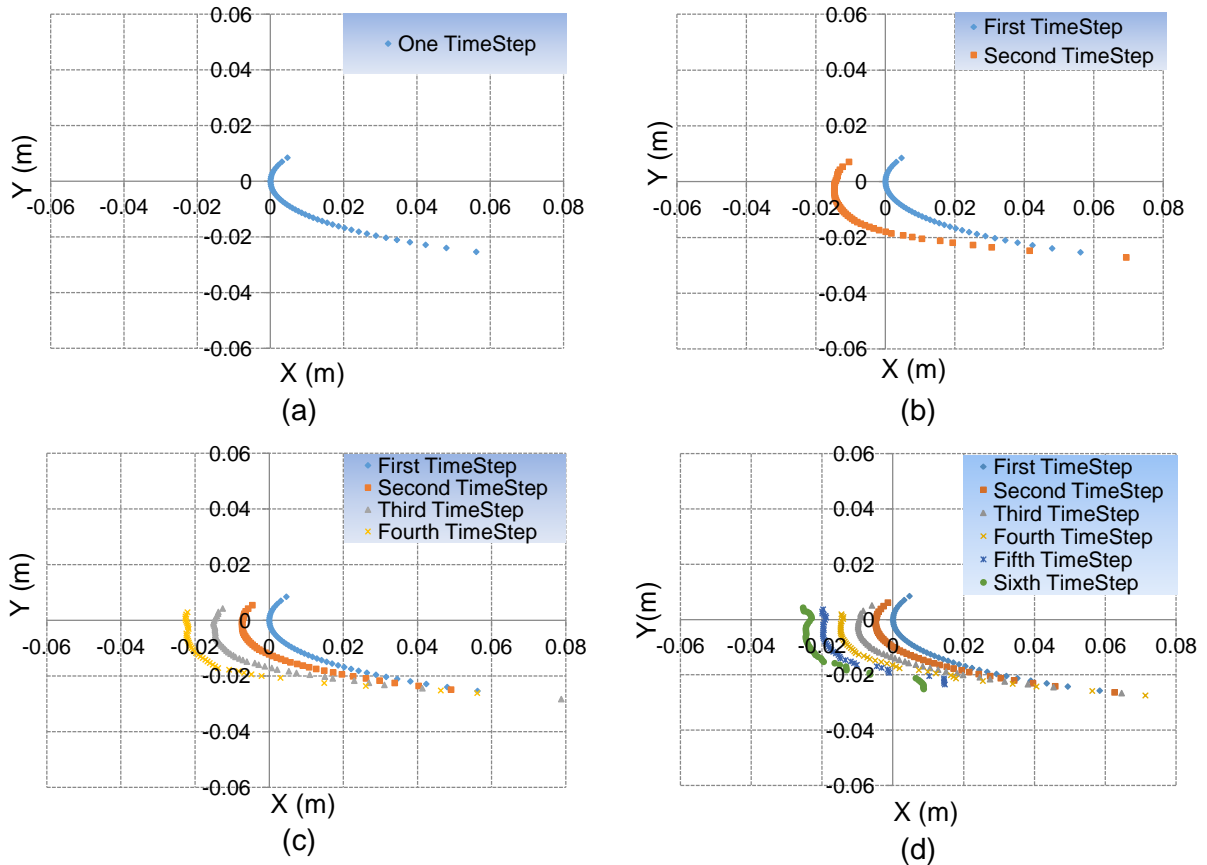


Figure 5: Location of impingement regions for Case-33 with a)one, b) two, c) four and d) six time steps

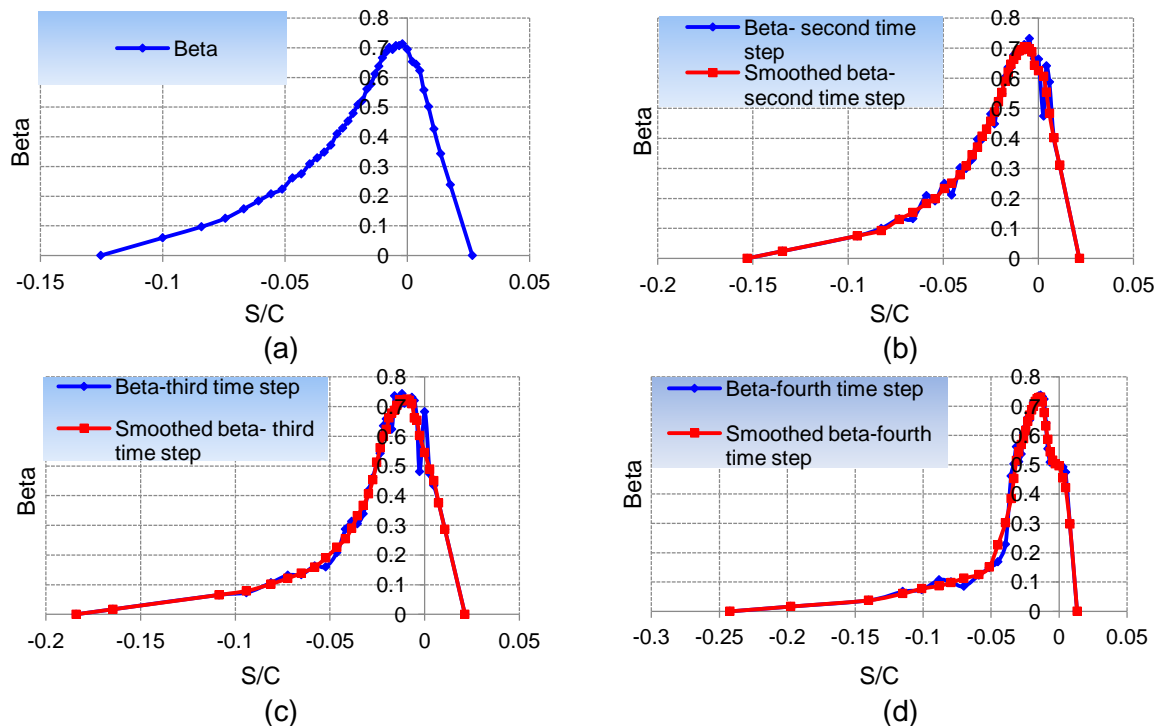


Figure 6: Collection efficiency for Case-27 with four time steps a) first time step, b) second time step, c) third time step, d) fourth time step

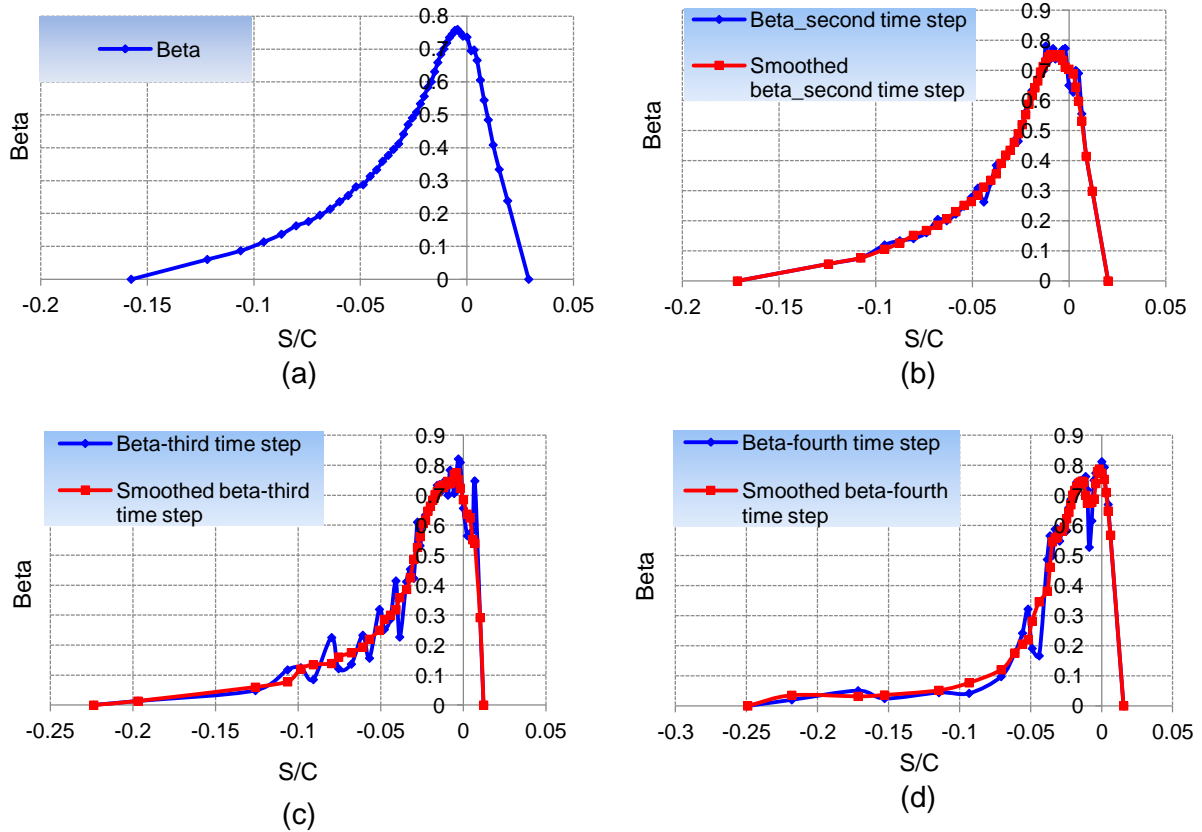


Figure 7: Collection efficiency for Case-33 with four time steps a) first time step, b) second time step, c) third time step, d) fourth time step

Ice Accretion Results

Thickness of rime ice is computed using the extended Messinger model [Myers, 2001] by the following equation:

$$\text{Rime ice thickness, } B = \frac{\beta \text{ LWC } V_{\text{inf}}}{\rho_r} t \quad (9)$$

where β is the collection efficiency parameter, LWC is the liquid water content, V_{inf} is the free stream velocity, t is the exposure time and ρ_r is the rime ice density. The shape of the ice accretion is obtained by calculating ice thickness value and plotting it in the normal vector direction for each surface panel on the impacting region. It is directly calculated for one time step and by repeating OpenFOAM computation procedure every time step for multi-time step cases.

Case-27:

Figures 8, 9, 10 and 11 show the comparison between ice shape predictions for Case-27 using OpenFOAM with the predictions of a commercial package FENSAP and the published experimental data in the literature [Wright et al., 1997]. The obtained ice shape using OpenFOAM with one time step computation is in good agreement in prediction of impingement limits and in poor agreement in prediction of ice shape and thickness compared with experimental results. Improvements of ice accretion shape and thickness are observed clearly with solving using two, four and six time steps.

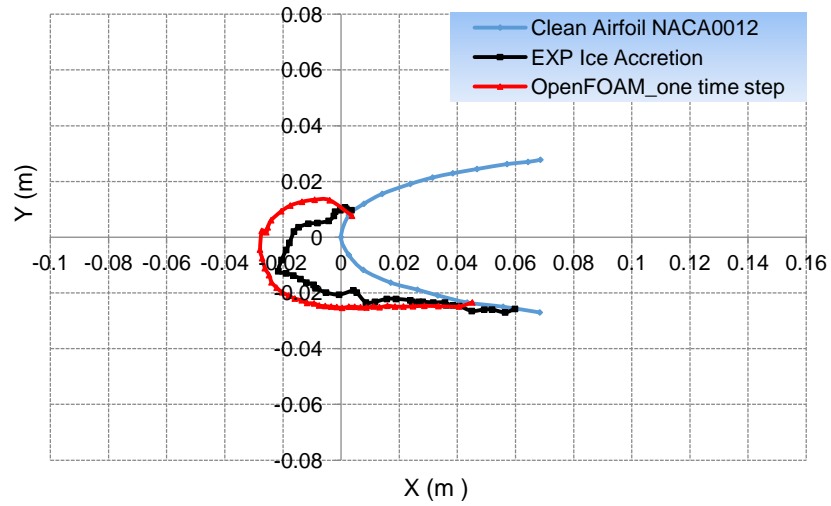


Figure 8: Comparison of rime ice accretion prediction using OpenFOAM with one time step and experimental data of NASA Case-27

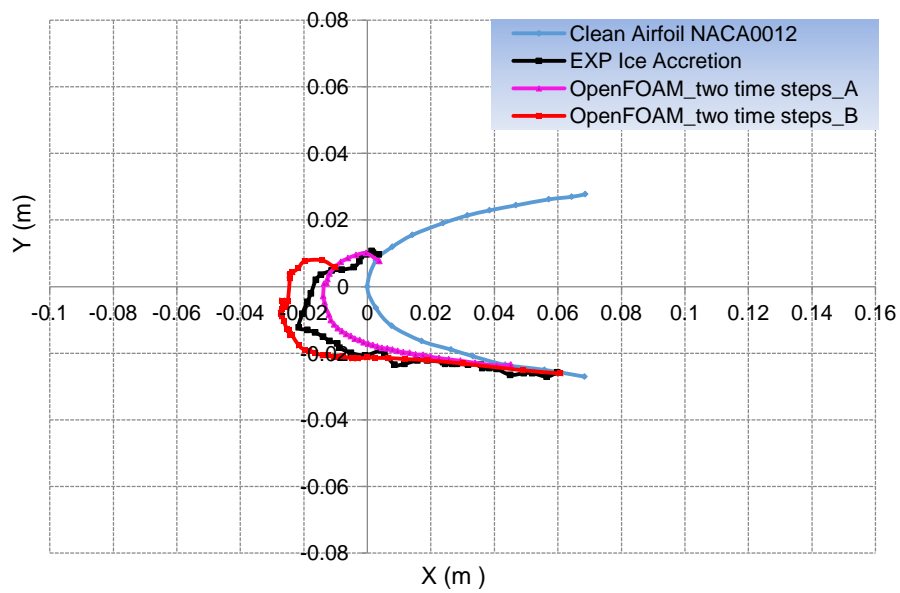


Figure 9: Comparison of rime ice accretion prediction using OpenFOAM with two time steps and experimental data of NASA Case-27

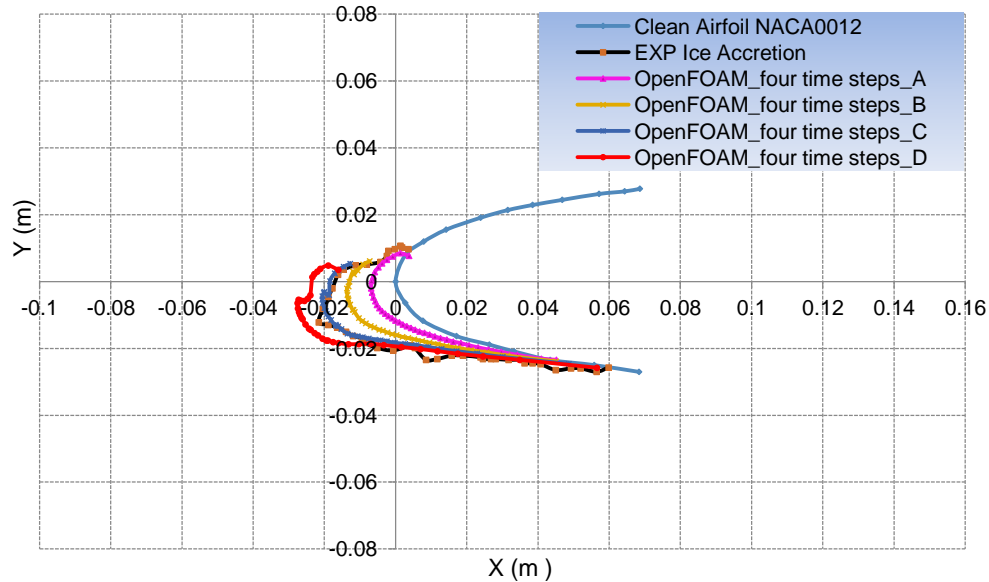


Figure 10: Comparison of rime ice accretion prediction using OpenFOAM with four time steps and experimental data of NASA Case-27

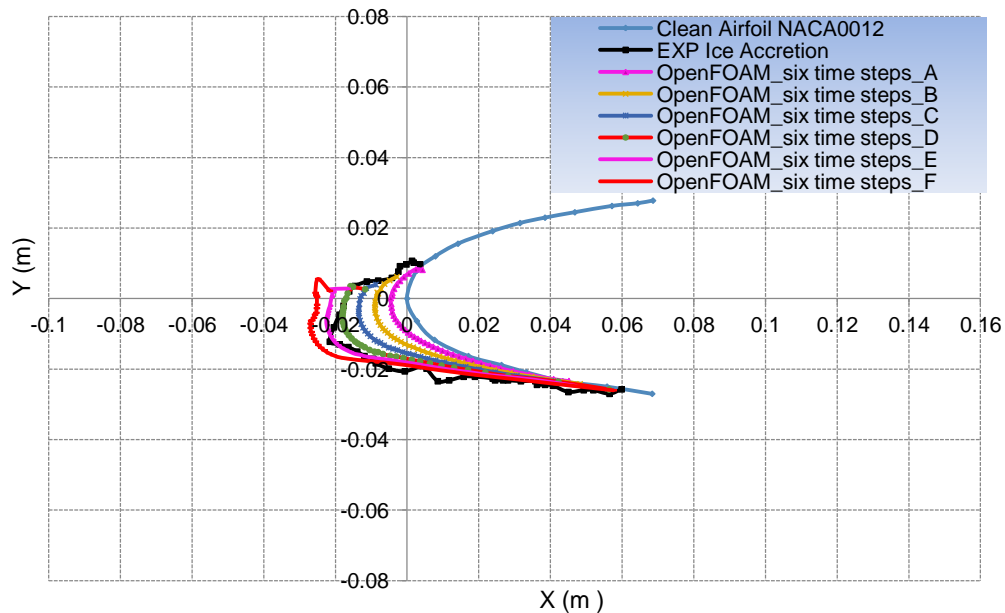


Figure 11: Comparison of rime ice accretion prediction using OpenFOAM with six time steps and experimental data of NASA Case-27

Case-33:

Figures 12, 13, 14 and 15 show the comparison between ice shape predictions for Case-33 using OpenFOAM with commercial package FENSAP predictions and published experimental data [Wright et al., 1997]. The obtained ice shape using OpenFOAM with one time step computation is also in good agreement in prediction of impingement limits. The ice shape and thickness are improved clearly with solving using two, four and six time steps compared with experimental results.

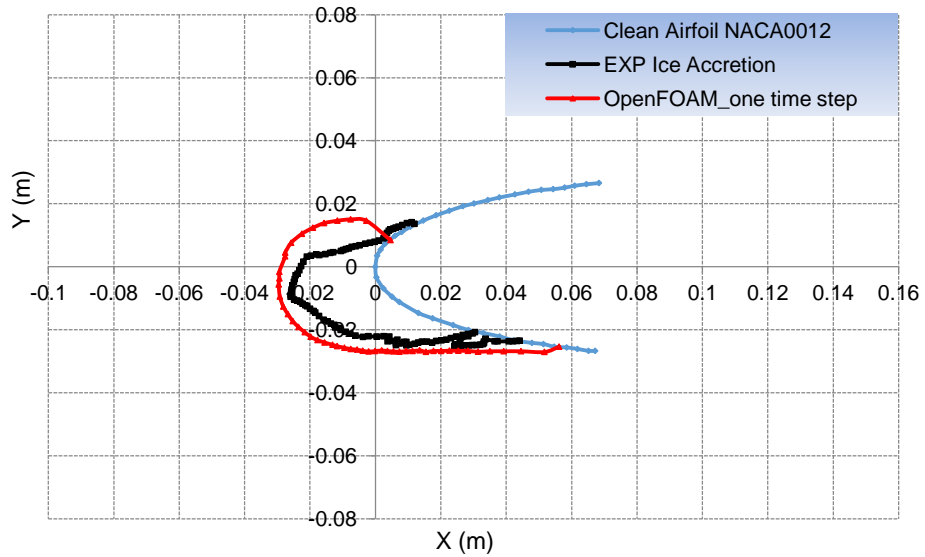


Figure 12: Comparison of rime ice accretion prediction using OpenFOAM with one time step and experimental data of NASA Case-33

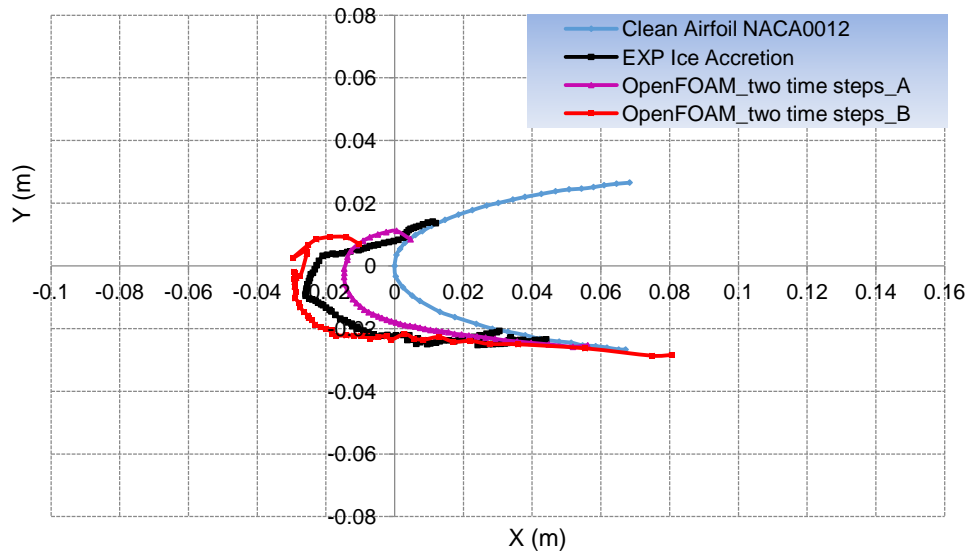


Figure 13: Comparison of rime ice accretion prediction using OpenFOAM with two time steps and experimental data of NASA Case-33

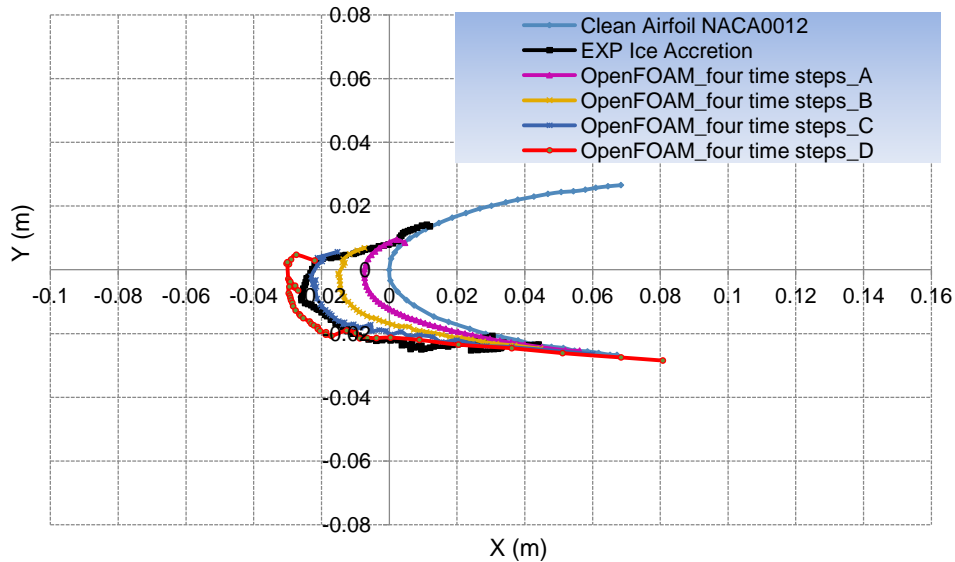


Figure 14: Comparison of rime ice accretion prediction using OpenFOAM with four time steps and experimental data of NASA Case-33

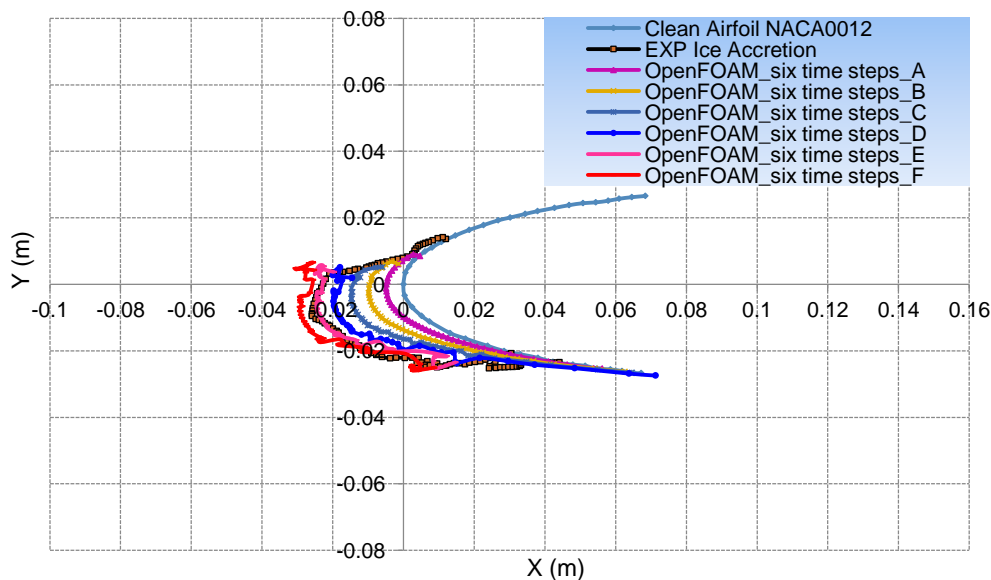


Figure 15: Comparison of rime ice accretion prediction using OpenFOAM with six time steps and experimental data of NASA Case-33

Comparison between OpenFOAM, FENSAP Predictions and Experimental Curves:

As expected ice shapes obtained by OpenFOAM with multi-time steps for both cases are more accurate than single time step. The improvement of ice shapes can be seen clearly when two time steps ice curves are compared with single time step ice shape curves. A similar behavior is observed when four time steps ice curves are compared with two time steps ice curves. Slight improvement in ice shapes and thicknesses is obtained with six time steps compared with four time steps.

Figures 16 and 17 show the obtained final predictions of rime ice shapes using OpenFOAM with four time steps for cases 27 and 33 respectively. OpenFOAM ice shape curves are compared with experimental ice shape and the ice shape predictions using ANSYS-FENSAP with four time steps for these cases.

The resulted rime ice shapes obtained using OpenFOAM with four time steps for both cases match the experimental ice curves along the lower and upper parts of the airfoil and have a slight overestimation at the airfoil leading edge.

Ice shape prediction obtained using the commercial ANSYS-FENSAP package [ANSYS, 2017]. FENSAP results with four time steps for cases 27 and 33 match the experimental data except at the airfoil leading edge, where FENSAP underestimates the ice thickness compared with experimental curves. Overall the OpenFOAM and FENSAP predictions with four time steps are reasonably accurate when compared with the experimental results.

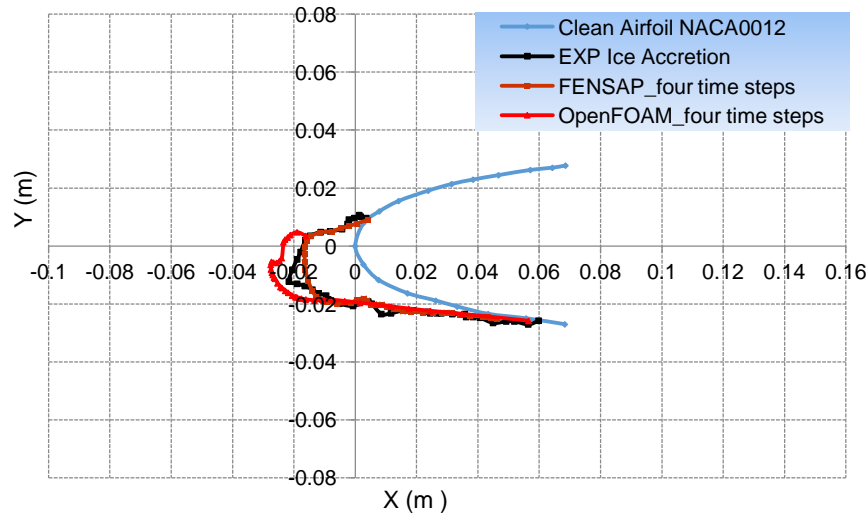


Figure 16: Comparison of rime ice accretion predicted using OpenFOAM with four time steps, FENSAP with four time steps results and experimental data of NASA Case-27

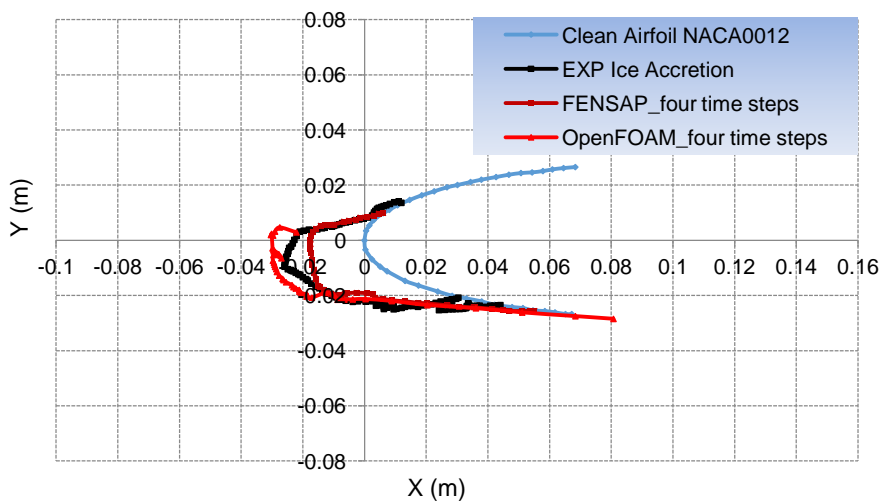


Figure 17: Comparison of rime ice accretion predicted using OpenFOAM with four time steps, FENSAP with four time steps results and experimental data of NASA Case-33

Effect of Iced Airfoil on Aerodynamic Coefficients

Case-27:

In-flight ice accretion on wings affects aerodynamic characteristics and aircraft performance. Rime ice which is formed on airfoil NACA 0012 for Case-27 takes the shape of the airfoil and does not affect significantly the lift and drag coefficients at small angles of attack as shown in Figures 18 and 19. Reduction of lift force coefficient of iced airfoil compared with clean airfoil

at different angles of attack is negligible because the formed rime ice does not produce extreme changes in the airfoil shape. Drag force coefficient increases gradually in negative angle of attack side as shown in Figure 19.

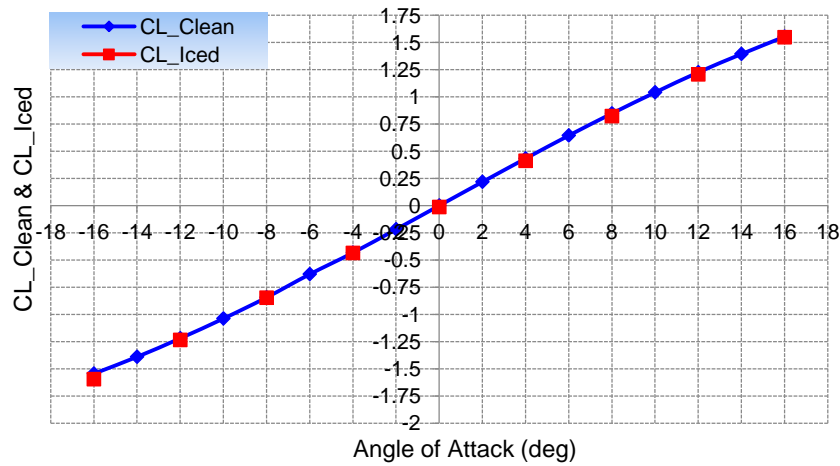


Figure 18: Effect of rime ice shape on lift coefficient of airfoil NACA 0012 for Case-27

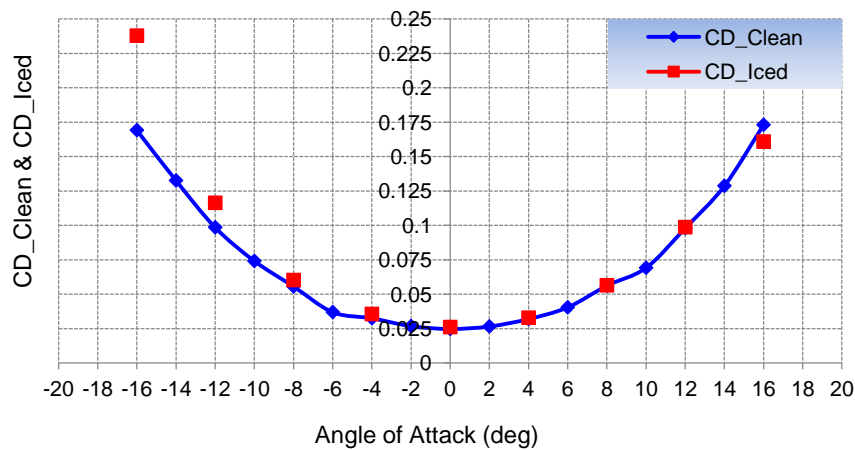


Figure 19: Effect of rime ice shape on drag coefficient of airfoil NACA 0012 for Case-27

Case-33:

Ice accretion on airfoil NACA 0012 for Case-33 takes also the shape of the airfoil. Its effect on reducing lift coefficient is negligible at different angles of attack. Drag coefficient of the iced airfoil is clearly increased as angle of attack increases in negative or positive directions. Figures 20 and 21 show the effect of rime ice accretion on lift and drag coefficient at different angles of attack.

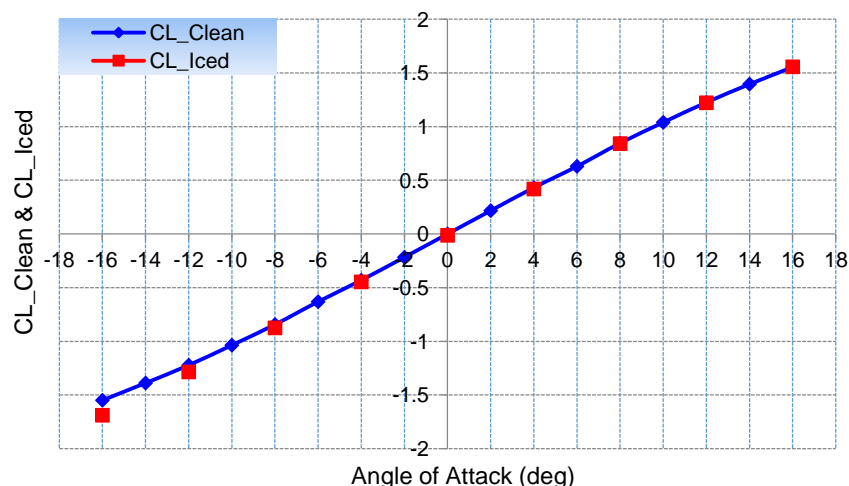


Figure 20: Effect of rime ice shape on lift coefficient of airfoil NACA 0012 for Case-33

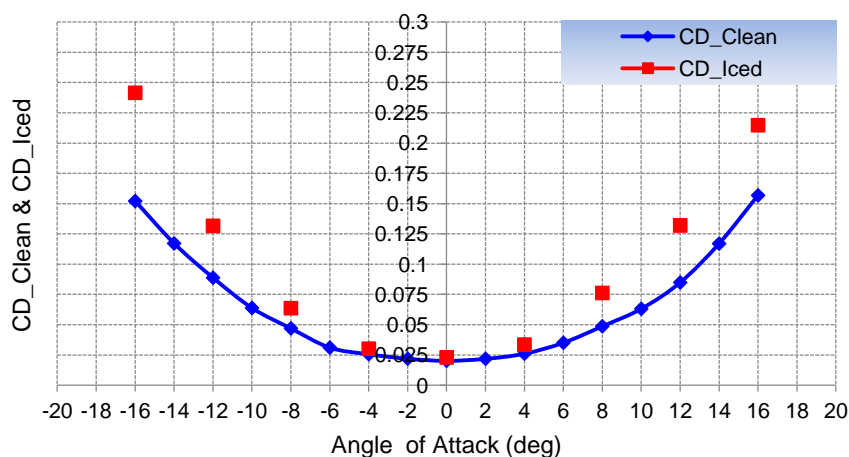


Figure 21: Effect of rime ice shape on drag coefficient of airfoil NACA 0012 for Case-33

CONCLUSION

Four modules of OpenFOAM have been integrated to simulate ice accretion on aerodynamic surfaces. These modules are fluid flow module, trajectory module, thermodynamic and ice calculation module, and geometry updating module. OpenFOAM simulations of rime ice accretion process on NACA 0012 airfoil and ice shape predictions for cases 27 and 33 of the DRA/NASA/ONERA collaborative icing research test cases [Wright et al., 1997] are performed successfully. The simpleFoam solver of OpenFOAM is used to simulate and solve the fluid flow with boundary conditions of both cases. Lagrangian approach in OpenFOAM is selected to simulate supercooled water droplet trajectories. Supercooled water droplets are released upstream far from airfoil leading edge and computing their trajectories using icoUncoupledKinematicParcelFoam solver until impacting the surfaces or escaping away from it. Droplet trajectories are computed based on Newton's second law under the effect of gravity, buoyancy, and drag forces. The coupling process between fluid flow solver simpleFoam and the trajectory solver icoUncoupledKinematicParcelFoam solver are developed and executed successfully.

The obtained ice shapes and ice thicknesses are in reasonably good agreement with literature data. The accuracy of using OpenFOAM software for rime ice shape prediction is improved clearly by simulation with multi-time steps. The effect of rime ice of the simulated cases on aerodynamic performance reveals that it has a negligible effect on lift force

coefficient due to its streamlined shape, but it increases drag force especially at high angles of attack. The obtained ice accretion results demonstrate that OpenFOAM solvers for mesh generation, fluid flow, trajectory integrated here with multi time step for ice formation have the capability to simulate rime ice accretion problems and give reasonably good predictions of ice shapes and thicknesses.

Acknowledgement

The authors would like to express their appreciations to Dr. Emre OZTURK and Mr. Semih TEKELIOGLU of ANOVA Engineering and Computer for making their ANSYS-FENSAP_ICE package training program available to the first author. Special thanks go to them for the guidance and help offered during the usage of the software. Thanks are also extended to the OpenFOAM community for making the OpenFOAM tools used in this work publicly available.

References

- Alzaili, J.S., (2012) *Semi-empirical approach to characterize thin water film behaviour in relation to droplet splashing in modelling aircraft icing*. Ph.D. Thesis, Cranfield University, England.
- ANSYS, Inc., (2017) *ANSYS FENSAP-ICE user tutorial guide*. Release 18.0.
- Beld, E., (2013) *Droplet impingement and film layer modeling as a basis for aircraft icing simulations in openfoam*. Internship Report, University of Twente, The Netherlands.
- Da Silveira, R.A., Maliska, C.R., Estivam, D.A., and Mendes, R., (2003). Evaluation of collection efficiency methods for icing analysis. Proceedings of 17th International Congress of Mechanical Engineering.
- Da Silveira, R.A., and Maliska, C.R. (2001) *Numerical simulation of ice accretion on the leading edge of aerodynamic profiles*. Proceeding of the 2nd International Conference on Computational Heat and Mass Transfer COPPE/UFRJ, Brazil.
- Greenshields, C.J. (2015) *OpenFOAM user guide*.
- Greenshields, C.J. (2015) *OpenFOAM programmers guide*.
- Gent, R.W., Dart, N.P., and Cansdale, J.T., (2000) *Aircraft icing*. Philosophical Transactions of the Royal Society of London A: Mathematical, Physical and Engineering Sciences. 358(1776): p. 2873-2911.
- Heinrich, A., (1991) *Aircraft icing handbook-Volume 1 of 3*. Atlantic City International Airport, NJ 08405: Department of Transportation, Federal Aviation Administration Technical Center. DOT/FAA/CT-88/8-1.
- Jasak, H., (2009) *OpenFOAM: open source CFD in research and industry*. International Journal of Naval Architecture and Ocean Engineering, 1(2), pp. 89-94.
- Ladson, C.L., (1988) *Effects of independent variation of Mach and Reynolds numbers on the low-speed aerodynamic characteristics of the NACA 0012 airfoil section*.
- Myers, T.G., (2001) *Extension to the Messinger model for aircraft icing*. AIAA journal, 39(2): p. 211-218.
- Rong, J., (1991) *Icing effects on a horizontal axis wind turbine*. Master's Thesis, Memorial University of Newfoundland, Canada.
- Wright, W.B., Gent, R.W., Guffond, D., (1997) *DRA/NASA/ONERA collaboration on icing research, Part II. Prediction of airfoil ice accretion*, NASA CR-202349.